Int. J. Heat Mass Transfer. Vol. 24, No. 11, pp. 1801-1810, 1981
Printed in Great Britain

0017-9310/81/111801-10 $02.00/0

AN ANALYSIS OF THE EFFECT OF PLATE THICKNESS ON LAMINAR FLOW AND HEAT TRANSFER IN INTERRUPTED-PLATE PASSAGES

S. V. PATANKAR and C. PRAKASH
Department of Mechanical Engineering, University of Minnesota, Minneapolis, MN 55455, U.S.A.

(*Received* 27 *January* 1981 *and in revised form* 8 *May* 1981)

Abstract—An analysis is presented for the flow and heat transfer in an interrupted-plate passage, which is an idealization of the offset-fin heat exchanger. The plates are considered to be of finite thickness. The effect of the plate thickness on the flow field and heat transfer is investigated through numerical solutions of the governing equations. The flow field is found to be quite complex. It contains recirculation zones behind the trailing edges of the plates, and there occurs significant deflection of the through flow. Whereas this greatly increases the pressure drop required for a given flow rate, the heat transfer from the thick plates does not improve sufficiently. Detailed results are presented for a number of thickness ratios and for a range of the Reynolds number. The overall results are compared with available experimental data.

NOMENCLATURE

A, total heat transfer area;
A_c, minimum flow area;
c_p, specific heat;
D_h, hydraulic diameter;
f, friction factor based on u_{av} and D_h, equation (15);
$\hat{f}$, friction factor based on $\hat{u}_{av}$ and $2H$, equation (7);
h, heat transfer coefficient, equation (26);
H, transverse spacing between the plates;
k, thermal conductivity;
L, plate length;
L_x, exchanger length;
LMTD, log-mean temperature difference, equation (23);
$\dot{m}$, total mass flow rate through the module;
p, pressure;
P, periodically varying part of pressure, equation (1);
Pr, Prandtl number;
Q, rate of total heat transfer from each plate;
q_{av}, average heat flux on a plate, equation (27);
Re, Reynolds number, equation (6) and (14);
St, Stanton number based on u_{av}, equation (28);
$\hat{St}$, nominal Stanton number based on $\hat{u}_{av}$, equation (29);
t, plate thickness;
T, temperature;
T_b, bulk temperature;
T_w, wall temperature of plate AB (Fig. 1);
$\tilde{T}$, periodically varying part of the temperature, equation (16);
ΔT, temperature difference between plates of successive ranks;
u, velocity in the x direction;
u_{av}, average velocity based on minimum flow area A_c;
$\hat{u}_{av}$, nominal average velocity based on transverse spacing between plates H, equation (5);
v, velocity in the y direction;
x, coordinate along the main flow direction;
y, transverse coordinate;
z, coordinate perpendicular to the plane of Fig. 1.

Greek symbols

β, overall pressure drop per unit length in the main flow direction;
μ, viscosity;
ρ, density.

INTRODUCTION

COMPACT heat exchangers are increasingly used in a wide variety of industrial applications. The offset-fin geometry, which is described in [1] and [2], appears to be most commonly employed. Figure 1 shows an array of interrupted plates, which can be regarded as a 2-dim. idealization of the offset-fin heat exchanger. It is well known that the plate interruptions cause a continual restarting of the thermal boundary layer, which results in high heat transfer coefficients. This improved heat transfer performance is, however, accompanied by larger pressure drop due to the restartings of the velocity boundary layer. Therefore, to optimize the heat exchanger design, reliable information is needed about both the heat transfer coefficient and the friction factor.

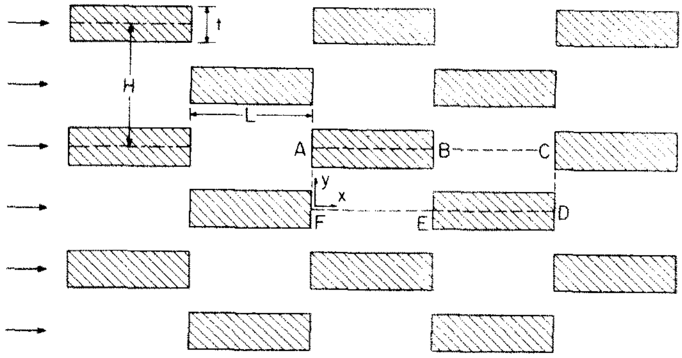

FIG. 1. An interrupted-plate passage.

Available experimental information on offset-fin surfaces has been presented, reviewed, and correlated in [1], [2], and [3]. Sparrow, Baliga, and Patankar [4] assumed the plate thickness t in Fig. 1 to be negligible and obtained numerical solutions for laminar flow and heat transfer for the resulting thin-plate passage.

The research described here focuses attention on the effect of plate thickness. It is believed that the finite thickness of the plates reduces the heat exchanger performance. Yet, there is no way in practice to avoid at least a certain minimum thickness of the plates, which is needed for structural integrity. This thickness may imply that the thickness ratio t/H is not negligible if the dimension H, shown in Fig. 1, is itself chosen to be small in the interest of compactness of the heat exchanger.

The study of the thickness effect is of interest in a number of other contexts. The plates used in practice often have bent, burred, or scarfed edges. Moreover, particle deposits and fouling can occur on the plates. These influences increase the effective thickness of the plates, and it is desirable to predict the corresponding degradation of performance. In addition to the offset-fin geometry, the flat-tube-and-plate-fin geometry [3] lends itself to the 2-dim. idealization shown in Fig. 1, where the thick plates can be imagined to be flattened tubes. Thus, the results of the present study are also relevant to the flat-tube heat exchangers.

The analysis of laminar flow in the thick-plate array presents a more difficult computational problem than the one solved in [4] for thin plates. When the plate thickness is neglected, the impingement region on the leading edge and the recirculating region behind the trailing edge are absent. Therefore, the analysis in [4] was performed by the use of a parabolic (i.e. boundary-layer type) procedure, in which the solution could be obtained by marching from the inlet plane to the successive locations downstream. The thick-plate analysis requires the solution of an elliptic problem, in which the downstream locations have a significant effect on the upstream happenings. Although calculation methods are available for such problems (for example, [5]), they require greater computer storage and time than their parabolic counterpart. It would, therefore, require excessive computing resources if an interrupted-plate passage involving many ranks of plates were to be analyzed. Fortunately, in passages of this kind, the flow attains a periodic fully-developed behaviour after a short entrance region, which may extend to about 5 (at the most, 10) ranks of plates [4]. In the periodic regime, the flow repeats itself in an identical manner for successive geometrical modules. The existence of this fully-developed periodic regime was first identified in [4]. Later, a calculation method was developed in [6], which could directly obtain the solution for a typical module, such as ABCDEFA in Fig. 1, without the need for the entrance-region calculation. For design purposes, it is sufficient to know the flow and heat transfer characteristics for such a typical module in the fully developed regime. For a heat exchanger consisting of a large number of modules, the somewhat different behaviour of the first few modules in the entrance region should be unimportant.

The present paper describes the analysis and results for the typical module shown in Fig. 1. The results are presented for different values of t/H and for a range of the Reynolds number. The plate spacing is kept constant at $L/H = 1$. The heat transfer results pertain to a Prandtl number of 0.7.

MATHEMATICAL FORMULATION

The velocity field

As mentioned earlier, the calculations for the periodic fully-developed flow will be confined to the typical module ABCDEFA, shown in Fig. 1. Here AC and FD are the lines of symmetry, while the flow across line AF should be identical to the flow across CD. The flow is assumed to be laminar and the fluid properties to be constant.

As explained in [6], the pressure p in periodic fully developed flows can be expressed by

$$p(x,y) = -\beta x + P(x,y), \tag{1}$$

where β is a constant, and $P(x,y)$ behaves in a periodic fashion from module to module. The term βx is indicative of the general pressure drop that takes place in the flow direction; $2\beta L$ gives the pressure drop over the module shown in Fig. 1. The flow in the module is governed by the continuity and momentum equations, which can be written as

$$\frac{\partial u}{\partial x}+\frac{\partial v}{\partial y}=0 \tag{2}$$

$$\rho\left(u\frac{\partial u}{\partial x}+v\frac{\partial u}{\partial y}\right)=\beta-\frac{\partial P}{\partial x}+\mu\left(\frac{\partial^2 u}{\partial x^2}+\frac{\partial^2 u}{\partial y^2}\right) \tag{3}$$

$$\rho\left(u\frac{\partial v}{\partial x}+v\frac{\partial v}{\partial y}\right)=-\frac{\partial P}{\partial y}+\mu\left(\frac{\partial^2 v}{\partial x^2}+\frac{\partial^2 v}{\partial y^2}\right) \tag{4}$$

The boundary conditions are provided by the no-slip requirement on the plate surface, by $v = 0$ and $\partial u/\partial y = 0$ on the symmetry lines BC and FE, and by the periodic behavior across AF and CD.

Since the boundary conditions do not involve the specification of any inflow velocities, the mass flow rate through the module cannot be directly prescribed. On the other hand, the pressure gradient β must be known so that equations (2)–(4) can be solved. In other words, one specifies the pressure drop for the module, and the resulting velocity field implies certain mass flow rate or the corresponding Reynolds number. In a computation, however, it is possible to iteratively adjust various quantities so that the converged solution is obtained for a given mass flow rate or Reynolds number.

With this understanding, the velocity field can be seen to be completely governed by three parameters: L/H, t/H and the Reynolds number.

When the plate thickness is significant, the variations in the flow area lead to different definitions of the Reynolds number and the friction factor. Some are more conventional, while other definitions may serve to display the effect of plate thickness more directly. For this reason, two sets of definitions are used here.

If $\dot{m}$ denotes the mass flow rate through the module per unit length in the z direction (normal to the plane of Fig. 1), an average velocity $\hat{u}_{av}$ can be based on the nominal width $(H/2)$ of the module. (The width $H/2$ corresponds to what is sometimes called the "frontal area" of the heat exchanger.)

Thus,

$$\hat{u}_{av}=\dot{m}/(\rho H/2). \tag{5}$$

Since the overall appearance of the interrupted-plate passage is akin to a parallel-plate channel of a nominal width H, the corresponding hydraulic diameter is $2H$. This leads to the definition of the Reynolds number as

$$Re=\rho\hat{u}_{av}(2H)/\mu=4\,\dot{m}/\mu. \tag{6}$$

The corresponding friction factor $\hat{f}$ is defined as

$$\hat{f}=\beta(2H)/(2\rho\hat{u}_{av}^2). \tag{7}$$

Whereas for thin plates $\hat{f}$ is a measure of only the wall friction, for thick plates $\hat{f}$ represents the total drag which includes the form drag as well as the friction drag.

The other set of definitions are constructed along the lines suggested by Kays and London [3]. The average velocity u_{av} is based on the minimum flow area A_c anywhere in the channel. Thus

$$u_{av}=\dot{m}/(\rho A_c), \tag{8}$$

where A_c is taken for the module in Fig. 1 per unit length in the z direction. The hydraulic diameter D_h is calculated from

$$D_h/L_x=4\,A_c/A, \tag{9}$$

where L_x is the x-direction length of the heat exchanger, and A is the heat transfer area in that length.

Exactly what expression should be used for A_c and A is somewhat arbitrary, and different practices seem to be employed by different workers. The practice of Kays and London, as inferred from the numerical values given for Fig. 10–53 of [3], appears to be to take A_c as $0.5\,(H-t)$ for the module chosen in Fig. 1. This is the flow area over most of the passage, but not the *minimum* area which occurs at line BE. In the calculation of the heat transfer area A, different practices may or may not include the extra area provided by the blunt edges of the plates. These seemingly unimportant differences in definitions do, however, have a significant impact on the correlation of friction-factor and heat transfer results.

In the present work, different combinations of practices were tried. The practices that are finally adopted are those that give the best correlation of the overall results for friction and heat transfer. No fundamental significance is attached to these particular practices.

Here the area A_c is taken to be the minimum flow area that occurs at line BE in Fig. 1. Thus,

$$A_c=0.5H-t \tag{10}$$

for a unit length in the z direction. In the calculation of the heat transfer area A, the extra area of the blunt edges of the plates is not included. For the module chosen here,

$$A=2L \tag{11}$$

for a unit length in the z direction, and

$$L_x=2L. \tag{12}$$

As a result,

$$D_h=2H-4t. \tag{13}$$

The Reynolds number Re can be obtained from

$$Re=\rho u_{av}D_h/\mu=4\,\dot{m}/\mu \tag{14}$$

which is the same as the Re given by equation (6). The friction factor is defined as

$$f=\beta D_h/(2\,\rho u_{av}^2). \tag{15}$$

It should be noted that, as the fin thickness t approaches zero, D_h becomes $2H$, and f and $\hat{f}$ become equal.

The temperature field

The heat transfer from the interrupted-plate array can be calculated for a variety of thermal boundary conditions. The calculation method for two kinds of boundary conditions was described in [6]. If all the plates are maintained at the same temperature, the bulk temperature of the fluid continuously gets closer to the plate temperature, and the modules in the far downstream region become virtually inactive. Thus, this boundary condition is unlikely to be employed in practice unless a significant temperature difference can be maintained everywhere between the fluid and the plates. Other common boundary conditions are those in which a uniform heat flux occurs along the plate surface or the plate temperature varies linearly in the flow direction. For simple fully-developed duct flows, these boundary conditions are easily attainable, because the flow conditions at the duct wall do not change in the streamwise direction. For the complex flow considered here, the expected variation of the local heat transfer coefficients precludes the possibility of establishing these simple boundary conditions in practice. A somewhat novel boundary condition is employed here, which appears to be practically relevant and attainable.

It is quite plausible that each plate provides the same rate of heat transfer Q (per unit length in the z direction) to the fluid. The distribution of this heat transfer in terms of the local heat flux and the local temperature along the length of the plate will depend on the flow conditions and the relative thermal resistance of the plate material. If this resistance is considered to be very small (implying a very high thermal conductivity of the plate material), the plate will attain a uniform temperature over its entire surface. Since the fluid temperature will increase in the flow direction, the successive plates must be maintained at increasing temperatures so as to enable each plate to transfer the same amount of heat to the fluid.

In practice, the plate temperature in an offset-fin heat exchanger is determined by the conditions at the side walls to which the fins are attached. For the purpose of analysis, it is convenient to imagine that an electric heater of power output Q is embedded in each plate of high thermal conductivity. Each plate will then attain a different uniform temperature, with a rising temperature pattern in the flow direction. Alternatively, the plates can be imagined to be flattened tubes, which carry another fluid. The temperature of this fluid in successive tubes is adjusted such that each tube experiences the same heat loss Q.

With this background, the thermal boundary condition used in this study can be envisaged as follows. All plates at a given streamwise location are at a uniform temperature, which exceeds by ΔT the temperature of the row of plates immediately upstream. Thus, for the module shown in Fig. 1, the plate AB is at a uniform temperature T_w, the next plate ED is at $T_w + \Delta T$, the plate starting at point C is at $T_w + 2\Delta T$, and so on. If each plate is to transfer the same amount of heat Q to the fluid, and if a thermally periodic state is to prevail, the mean fluid temperature would also rise by ΔT from station AF to station BE, and again by ΔT from BE to CD, and so on.

Since the fluid temperature T would, in general, rise in the flow direction, it does not behave in a periodic fashion. It is, therefore, convenient to express T as

$$T(x, y) = (x/L)\Delta T + \tilde{T}(x, y), \tag{16}$$

where $\tilde{T}(x, y)$ would vary periodically from module to module. The similarity between equations (1) and (16) is worth noting.

The energy equation can now be written as

$$\rho c_p\left(u\frac{\partial \tilde{T}}{\partial x} + v\frac{\partial \tilde{T}}{\partial y}\right) = -\rho c_p u\left(\frac{\Delta T}{L}\right) + \frac{\partial}{\partial x}\left(k\frac{\partial \tilde{T}}{\partial x}\right) + \frac{\partial}{\partial y}\left(k\frac{\partial \tilde{T}}{\partial y}\right) + \left(\frac{\Delta T}{L}\right)\frac{\partial k}{\partial x}. \tag{17}$$

Although the fluid conductivity k will be regarded as constant, the variable conductivity form of the energy equation is written here for a special purpose, which will be explained later.

The boundary conditions are given by $\partial \tilde{T}/\partial y = 0$ across BC and FE, by the periodic behaviour across AF and CD, and by the following variations along the plates AB and ED:

$$\text{Plate AB:}\quad \tilde{T} = T_w - (x/L)\Delta T, \tag{18}$$

$$\text{Plate ED:}\quad \tilde{T} = T_w + \Delta T - (x/L)\Delta T. \tag{19}$$

Here x is measured from point F. Equations (18) and (19) specify that $\tilde{T}$ varies from T_w to $T_w - \Delta T$ along each plate, thus confirming the periodic character of $\tilde{T}$.

For a given T_w (reference level) and a given ΔT (scaling factor), equation (17) can be solved in conjunction with the boundary conditions just stated. The resulting solution will describe the corresponding variation of the fluid temperature.

To express the heat transfer results in convenient dimensionless form, a number of related quantities will now be defined. The bulk temperature of the fluid is given by

$$T_b = \int T|u|\,dy / \int |u|\,dy, \tag{20}$$

where the integrals are to be carried over the y direction width of the module. The absolute value of u is taken so that the regions with reverse flow are also properly represented. As already mentioned, the values of T_b for locations AF, BE and CD in Fig. 1 are related by

$$(T_b)_{BE} = (T_b)_{AF} + \Delta T, \tag{21}$$

$$(T_b)_{CD} = (T_b)_{BE} + \Delta T. \tag{22}$$

To define the heat transfer coefficient for the plate AB, the appropriate wall-to-bulk temperature difference is the log-mean temperature difference given

$$\text{LMTD} = \frac{[T_w - (T_b)_{AF}] - [T_w - (T_b)_{BE}]}{\ln\{[T_w - (T_b)_{AF}]/[T_w - (T_b)_{BE}]\}} \tag{23}$$

This expression can be simplified by the use of equations (24) and (25) to read

$$\mathrm{LMTD} = \Delta T/\ln\{1+\Delta T/[T_w-(T_b)_{\mathrm{BE}}]\}. \quad (24)$$

It can be seen that the LMTD for plate ED can be similarly defined in terms of $(T_b)_{\mathrm{CD}}$ at its downstream end.

If Q denotes the heat lost by each plate (per unit length in the z-direction), the total heat input to the chosen module, which contains two half plates, is also Q. This causes a bulk temperature rise of $2\Delta T$ over the module. Therefore.

$$Q = 2\Delta T\dot{m}c_p. \quad (25)$$

The heat transfer coefficient can be calculated from

$$h = (Q/A)/\mathrm{LMTD}. \quad (26)$$

The average heat flux over the *entire* surface of the plate is, however, given not by Q/A but by

$$q_{av} = Q/(2L+2t). \quad (27)$$

Finally, the Stanton number follows from

$$St = h/(\rho c_p u_{av}). \quad (28)$$

An alternative Stanton number $\hat{St}$ can be based on the nominal average velocity $\hat{u}_{av}$ thus,

$$\hat{St} = h/(\rho c_p \hat{u}_{av}). \quad (29)$$

It should be noted that the heat transfer results presented in this paper correspond to the particular thermal boundary condition chosen here. Although the influence of different boundary conditions was not investigated, an estimate can be made from the well known results for a parallel-plate channel. It is expected that different thermal boundary conditions may produce about 10% difference in the predicted St values.

Computational details

The basic calculation method for periodic fully-developed flow has been adequately described in [6]. The same general method was used in the present investigation, although the solution of the velocity field was accomplished by the "SIMPLER" procedure [5]. This resulted in significantly faster convergence of the iteration process. The convergence was further speeded up by supplementing the line-by-line solution of the discretization equations by the additive–correction method of Settari and Aziz [7].

Rather than confine the computations to the rather irregular flow domain shown in Fig. 1, it seemed convenient to use the full rectangle ACDF as the calculation domain, which includes the region occupied by the solid plates as well as the region through which the fluid flows. A suitable method for incorporating such solid–fluid regions in one calculation domain has been developed in [8]. The solid regions are effectively treated by setting the viscosity there equal to a very large number.

In the solution of the temperature field, the conductivity for the solid regions should, in general, be set equal to the true conductivity of the solid. However, for the thermal boundary condition considered here, the uniformity of the plate temperature could be achieved by letting the solid region conductivity also to be equal to a very large number. At this point, it may be remembered that equation (17) was written for a variable conductivity situation. Although k can be taken to be constant within the solid and within the fluid, the last term in equation (17) would be non-zero, and must be correctly accounted for, at the solid–fluid interfaces normal to the x direction.

All computations were performed on a 60×30 grid. The x-direction grid spacing was varied so as to provide a fine grid near the leading and trailing edges of the plate. The y-direction grid was also made finer near the plate surfaces. Exploratory solutions on coarser grids and on grids with different grid-point distributions indicated that the presented results are accurate to at least 0.5%. The flow-field results for the case of zero plate thickness were found to agree perfectly with those of [4].

Computations were carried out for the thickness ratios $t/H = 0, 0.1, 0.2, 0.3$, and for the plate length given by $L/H = 1$. The Prandtl number was set equal to 0.7, while the Reynolds number Re was varied from 100 to 2000. In this range of Re, the real flow is expected to be mostly laminar, although it is possible that transition to turbulence may occur somewhat before $Re = 2000$ especially for the higher values of t/H. Also, the real flow may display instabilities and vortex-shedding from the trailing edges of the plates. These phenomena are beyond the scope of the present analysis.

The solution of equations (2)–(4) for a given value of Re was obtained as follows. The pressure gradient β was set equal to a convenient constant value (for example, $\beta = 1$). The first iteration for solving the flow equations was performed with a tentative value of the fluid viscosity μ. The resulting velocity field was used to calculate u_{av}. The viscosity μ was then recalculated such that the value of v_{av} would imply the given Re. Such iterative updating of μ finally led to the converged solution for the required value of Re.

RESULTS AND DISCUSSION

Flow field

Considerable insight into the behaviour of friction factor and heat transfer can be obtained from the calculated flow field. The streamline plots in Fig. 2 show how the flow pattern changes with increasing Reynolds number. The case of $t/H = 0.3$ is chosen so that the plate-thickness effect is particularly magnified. For the lower Reynolds numbers ($Re = 100$ and 500), there is an impingement flow on the leading edge of the plate and a small recirculation zone behind the trailing edge. The main flow is deflected quite significantly and

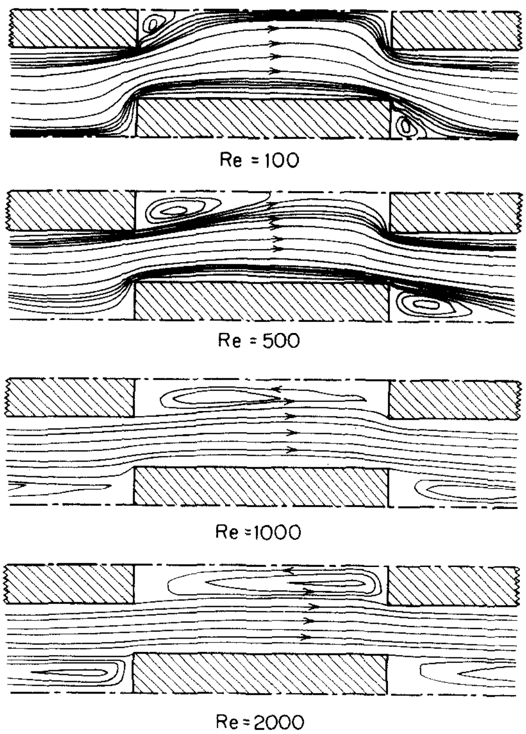

FIG. 2. Flow patterns for t/H = 0.3 at different Reynolds numbers.

has a tendency to move away from the main surface of the plate. For Re = 1000 and 2000, the recirculating flow fills the space between the trailing edge of one plate and the leading edge of the next plate, and the impingement flow disappears. At Re = 2000, the recirculation zone is seen to be shifted in the downstream direction. The through flow confines itself to the unobstructed central core of minimum cross-section and more-or-less aligns with the x direction.

The effect of various plate thicknesses on the flow pattern at a fixed Reynolds number (Re = 2000) is shown in Fig. 3. Here, for t/H = 0.1 and 0.2, the flow behavior is similar to the low Reynolds number cases in Fig. 2. Only when the plate is sufficiently thick, the recirculation zone extends to the next plate.

An interesting observation that can be made from Figs. 2 and 3 is that the area A_c given by equation (10) is indeed the minimum area experienced by the flow.

Friction factor

Here the friction factor is a measure of the pressure drop required to sustain the flow through the interrupted-plate array. The top diagram in Fig. 4 shows the variation of f with Re. The definition of f employed here has the ability to correlate the results in a somewhat narrow band. The $f \sim Re$ curves for different values of t/H in Fig. 4 can be seen to lie fairly close to each other.

It is not useful to focus attention on whatever dependence of t/H is noticeable in the top diagram of Fig. 4. The displayed dependence is strongly controlled by the definitions of A_c and A. If the practices of Kays and London [3] were used, then the $f \sim Re$ curves in Fig. 4 for different values of t/H would—it is possible to show—spread out quite significantly. Some definitions can show that f increases with t/H, while others show a decrease. It, therefore, appears that f is not a very useful quantity for the present problem since it is so sensitive to how D_h and u_{av} are defined.

By what factor does the pressure drop increase as a result of replacing the zero-thickness plates by plates of finite thickness? Such a question is not directly

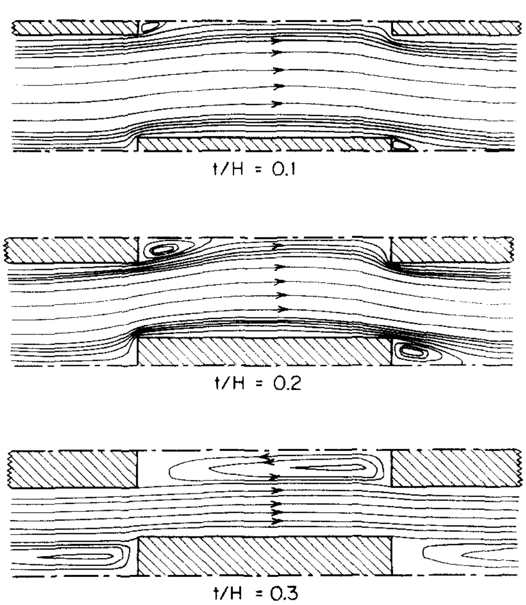

FIG. 3. Flow patterns for Re = 2000 for different plate thicknesses.

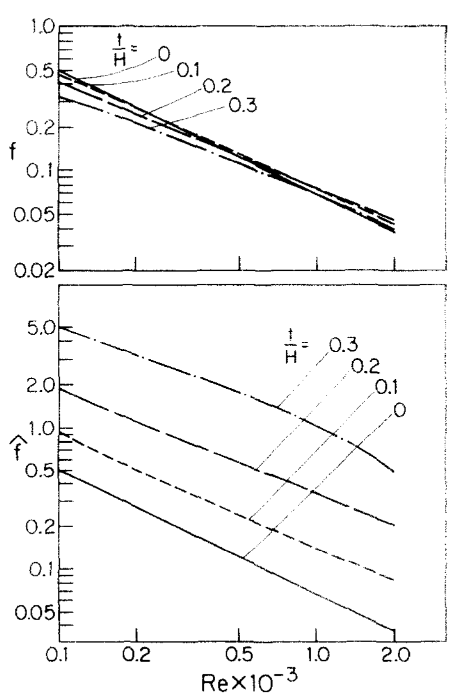

FIG. 4. Variation of the friction factor.

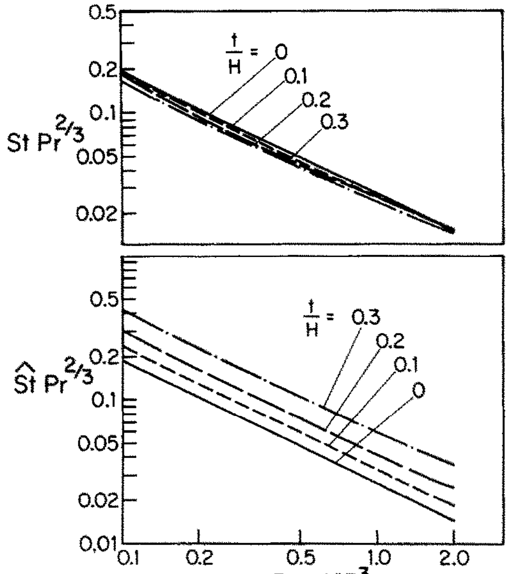

FIG. 5. Variation of the Stanton number.

answered by the $f \sim Re$ plot, because the plate thickness enters the definition of f through D_h and u_{av}. For this reason, the bottom diagram in Fig. 4 is provided. Here, at a given value of Re, $\hat{f}$ is a direct measure of the pressure drop for a given mass flow rate through a heat exchanger of fixed overall dimensions. Over the Reynolds number range shown, $\hat{f}$ for the thick plate ($t/H = 0.3$) is 10–16 times the corresponding values for the zero-thickness plate.

Overall heat transfer

The heat transfer results are presented in Fig. 5 in terms of $St\ Pr^{2/3}$ and $\hat{St}\ Pr^{2/3}$. The Prandtl number influence is included in the ordinate in an attempt to generalize the results to other fluids, although the present computations were performed only for $Pr = 0.7$. In the top plot of Fig. 5, St is seen to correlate very well with Re, with no significant influence of t/H. It should be remembered that the area of the blunt edges of the plates was not included in the heat transfer area A. What seems to happen is that the heat transfer from the blunt edges is rather small; and this extra heat transfer is just enough to compensate for the deterioration of the heat transfer from the main surface of the plate. The trailing edge of the plate is always rather inactive due to the separated flow there. As t/H or Re increases, even the leading edge is washed by the slow recirculating flow. The flow deflection away from the main surface of the plate causes some decrease of heat transfer there. Especially, the thin thermal boundary layer near the leading edge is considerably disturbed by the flow deflection in that region.

A direct comparison of the heat transfer from thick and thin plates can be made from the bottom plot in Fig. 5. Here, a given value of Re implies a fixed mass flow rate in the same overall geometry. Further, if the same temperature difference is allowed to exist between the fluid and the plates, $\hat{St}$ serves as a measure of the actual heat transfer from the plates. This heat transfer is seen to increase with t/H, but not as much as one would expect from the increased u_{av} and the increased surface area for the thick plates. The $\hat{St}$ values for the case of $t/H = 0.3$ are only about 2.4 times the corresponding values for the zero-thickness plate. The degradation is caused by the factors already discussed. Further, these $\hat{St}$ ratios must viewed in conjunction with the much higher ratios (10–16) for $\hat{f}$.

Comparison with experiment

A convenient way of comparing the present results with experimental data would have been to use the empirical correlations of Wieting [2]. However, these correlations are based on 3-dim. offset-fin configurations, with a finite dimension in the z direction. Further, the underlying data are all for rather small values of t/H with the result that Wieting does not include t/H as a parameter in his correlations for Reynolds numbers less than 1000. The data presented by London and Shah [1] also could not be used, since they do not include L/H values close to unity.

Comparisons are, therefore, made with the data from Fig. 10–53 of Kays and London [3]. For this case, the geometrical parameters are: $L/H = 1.14$, $t/H = 0.05$, and the z direction width is about $5.9\,H$. Thus the experimental situation corresponds only approximately to the one computed here. Further, it is stated in [3] that the offset-fin surfaces used in the experiments had burred edges. Finally, the heat transfer results may not be exactly comparable because of the differences in thermal boundary conditions. Kays and London [3] used condensing steam, leading to nearly uniform plate temperatures.

The different definitions of A_c, A, and D_h present a problem in this comparison. The difficulty can be totally avoided by working with $\hat{f}$ and $\hat{St}$ which are free

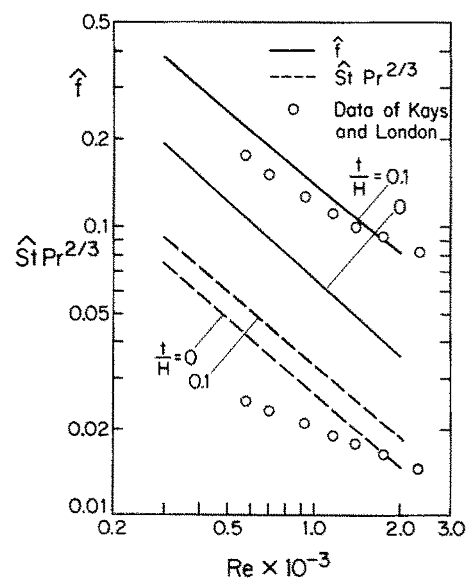

FIG. 6. Comparison with experimental data.

from the subtleties of definition. Figure 6 shows the results for $\hat{f}$ and $\hat{St}\, Pr^{2/3}$ plotted as a function of Re. The numerical results are shown for $t/H = 0$ and 0.1. The Kays and London data, which correspond to $t/H = 0.05$, have been appropriately converted to the coordinates of Fig. 6.

The agreement of the computed $\hat{f}$ values with the data can be judged to be quite satisfactory. The rather high values of $\hat{f}$ in the data for $Re = 1000$ may be due to turbulence. Also, the burred edges may imply a higher effective value of t/H.

There does not seem to be an obvious explanation for the poor agreement of the Stanton number results. Some departures between the experimental set-up and the numerical model have already been mentioned; but they alone may not be responsible for the large discrepancy between the data and the computations. The substantially different slopes of the data and the computed curves may be particularly disturbing. In this connection, one may wonder whether there is something peculiar about this particular data set of Kays and London. Many of their other data sets, albeit for different geometries, show that the slopes of the f and St curves are nearly equal. The equal slopes are also in evidence in most of the data presented by London and Shah [1], where they show the ratio of f to St to be nearly independent of the Reynolds number. Incidentally, the equal-slope behavior is indicated by the Reynolds analogy. In Fig. 6, whereas the computed curves for $\hat{f}$ and $\hat{St}$ do show nearly equal slopes, the experimental data for $\hat{St}$ seem to follow a less steeper line.

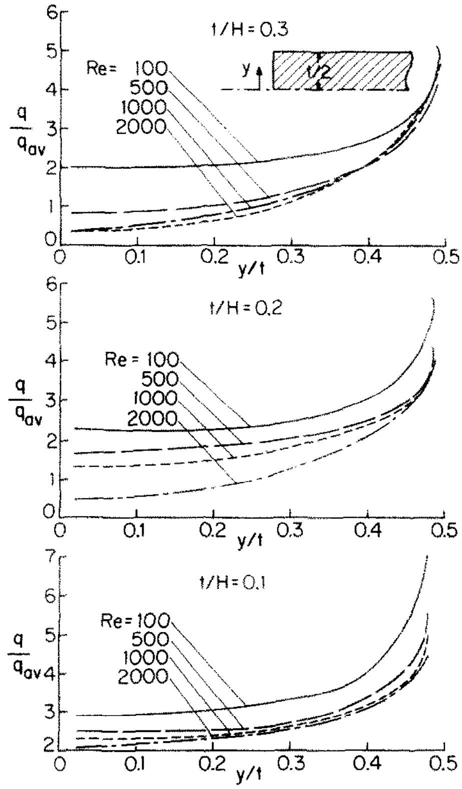

FIG. 8. Heat flux variation on the leading edge.

Local heat transfer

Further insight into the heat transfer behavior can be obtained by examining the variation of the local heat transfer along the surface of the plates. Figure 7 shows the variation of the local heat flux q along the main surface of the plates, such as the lower surface of plate AB in Fig. 1. Here q is normalized with reference to q_{av} which stands for the average heat flux over the entire surface of the plate. The variations in Fig. 7 show the influence of t/H and Re. In all cases, there is a large value of q/q_{av} near the leading edge of the plate (i.e. for small x/L) associated with the thin thermal boundary layer there. The rise in q/q_{av} near $x/L = 1$ is a result of the flow acceleration caused by the blockage effect of the next plate. The minimum value of q/q_{av} for each

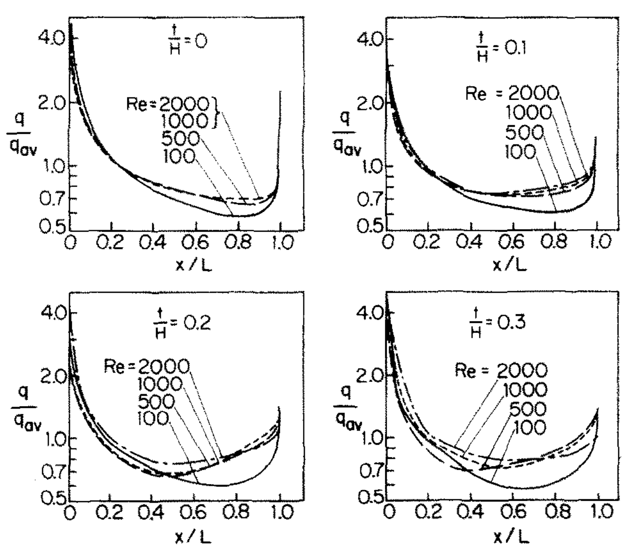

FIG. 7. Streamwise variation of the local heat flux.

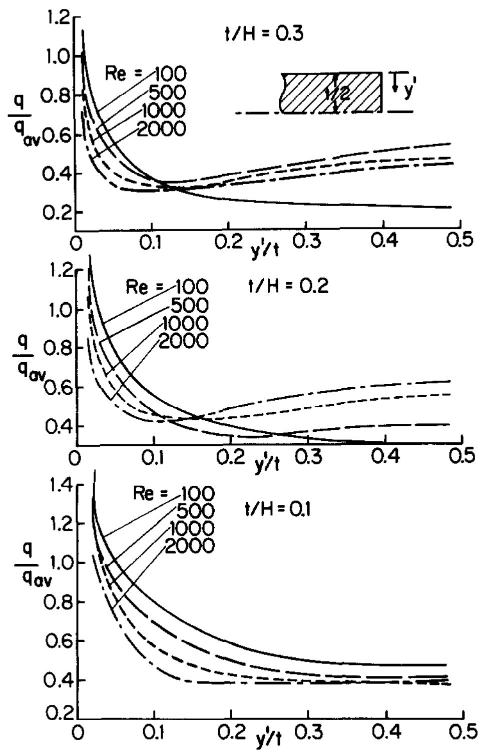

FIG. 9. Heat flux variation on the trailing edge.

Reynolds number appears to occur where, as seen from Figs. 2 and 3, the largest flow area is available for the through flow.

The variation of the local heat flux on the leading edge is shown in Fig. 8, while that on the trailing edge is plotted in Fig. 9. In general, the values of q/q_{av} on the leading edge are much greater than those on the trailing edge. In both figures, high heat transfer rates are found close to the sharp corner of the plate. Finally, higher Reynolds numbers seem to make the heat flux distribution more uniform.

CONCLUDING REMARKS

An analysis has been presented for the flow and heat transfer in an interrupted-plate passage, in which the plate thickness is significant. The finite-thickness plates are found to give rise to a complex flow pattern involving impingement and recirculation zones and flow deflection. Compared to the case of zero-thickness plates, the thick-plate situation leads to significantly higher pressure drop, while the heat transfer does not sufficiently improve despite the increased surface area and increased mean velocity.

Acknowledgement—This research was performed under the auspices of NSF Grant NSF/CME 8007476. Thanks are due to Professor Ralph L. Webb for some helpful suggestions.

REFERENCES

1. A. L. London and R. K. Shah, Offset rectangular plate-fin surfaces—heat transfer and flow friction characteristics, *J. Engng Power* **90**, 218–228 (1968).
2. A. R. Wieting, Empirical correlations for heat transfer and flow friction characteristics of rectangular offset-fin plate–fin heat exchangers, *J. Heat Transfer* **97**, 488–490 (1975).
3. W. M. Kays and A. L. London, *Compact Heat Exchangers* (2nd edn), McGraw–Hill, New York (1964).
4. E. M. Sparrow, B. R. Baliga, S. V. Patankar, Heat transfer and fluid flow analysis of interrupted-wall channels, with application to heat exchangers, *J. Heat Transfer* **99**, 4–11 (1977).
5. S. V. Patankar, *Numerical Heat Transfer and Fluid Flow*, McGraw–Hill, New York (1980).
6. S. V. Patankar, C. H. Liu and E. M. Sparrow, Fully developed flow and heat transfer in ducts having streamwise-periodic variation of cross-sectional area, *J. Heat Transfer* **99**, 180–186 (1977).
7. A. Settari and K. Aziz, A generalization of the additive correction methods for the iterative solution of matrix equations, *SIAM Jl Numerical Analysis* **10**, 506–521 (1973).
8. S. V. Patankar, A numerical method for conduction in composite materials, flow in irregular geometries and conjugate heat transfer, *Proc. 6th Int. Heat Transfer Conf., Toronto* **3**, 297 (1978).

ANALYSE DE L'EFFET DE L'EPAISSEUR DE LA PLAQUE SUR L'ECOULEMENT LAMINAIRE ET LE TRANSFERT THERMIQUE DANS DES PASSAGES DE PLAQUE INTERROMPUE

Résumé—On présente une analyse de l'écoulement et du transfert thermique dans un passage de plaque interrompue qui est l'idéalisation de l'échangeur à ailettes. Les plaques sont considérées à épaisseur finie. L'effet d'épaisseur sur le champ d'écoulement et sur le transfert thermique est étudié à travers la solution numérique des équations de base. Le champ d'écoulement est trouvé très compliqué. Il comprend des zones de recirculation derrière les bords de fuite des plaques et il y a aussi une déflexion marquée de l'écoulement. Tandis que cela accroit fortement la perte de pression pour un débit donné, le transfert de chaleur des plaques épaisses n'est pas suffisamment accru. Des résultats détaillés sont présentés pour un certain nombre de rapports d'épaisseur et pour un domaine de nombre de Reynolds. Les résultats sont comparés aux données expérimentales disponibles.

BERECHNUNG DES EINFLUSSES DER PLATTENDICKE AUF DIE LAMINARE STRÖMUNG UND DEN WÄRMEÜBERGANG IN KANÄLEN MIT UNTERBROCHENEN PLATTEN

Zusammenfassung — Es wird eine Berechnungsmöglichkeit für die Strömung und den Wärmeübergang in einem Kanal mit unterbrochenen Platten angegeben. Diese Anordnung stellt die Idealisierung eines Wärmeübertragers mit versetzten Rippen dar. Die Plattendicke wird als endlich betrachtet. Der Einfluß der Plattendicke auf das Strömungsfeld und auf den Wärmeübergang wird durch numerische Lösung der Bestimmungsgleichungen untersucht. Das Strömungsfeld stellt sich als sehr verwickelt dar. Es enthält Rückströmzonen hinter den Abströmkanten der Platten, wo auch eine erhebliche Ablenkung der freien Strömung auftritt. Während hierdurch der Druckabfall für einen vorgegebenen Massenstrom bei dicken Platten stark ansteigt, erhöht sich der Wärmeübergang dabei jedoch nur mäßig. Detaillierte Ergebnisse werden für eine Reihe von Dickenverhältnissen und Reynolds-Zahlen angegeben und mit bekannten experimentellen Daten verglichen.

АНАЛИЗ ВЛИЯНИЯ ТОЛЩИНЫ ПЛАСТИНЫ НА ЛАМИНАРНОЕ ТЕЧЕНИЕ И ТЕПЛОПЕРЕНОС В ЗАЗОРЕ МЕЖДУ ОТРЕЗКАМИ ПЛАСТИН

Аннотация — Проведен анализ течения и теплопереноса в зазоре между отрезками пластин. Рассматриваемый случай является идеализацией теплообменника со смещенными ребрами. Предполагается, что пластины имеют конечную толщину. Исследование влияния толщины пластины на поле течения и теплоперенос проводится на основе численного решения уравнений. Показано, что картина течения является довольно сложной. Она состоит из рециркуляционных зон за кромкой пластин, где наблюдается значительное отклонение основного потока. Несмотря на то, что это приводит к возникновению большого перепада давления, определяемого величиной расхода, количество тепла, переносимого от пластин большой толщины, существенно не увеличивается. Представлены подробные результаты для различных отношений толщин и значений числа Рейнольдса. Результаты расчета сравниваются с имеющимися экспериментальными данными.